https://doi.org/10.5194/egusphere-2024-3471
Preprint. Discussion started: 25 November 2024

Rapid Increases of Ozone Concentrations over Tibetan Plateau Caused by Local and Non-Local Factors

Chenghao Xu[1], Jintai Lin[1, 2], Hao Kong[1], Junli Jin[3], Lulu Chen[4], Xiaobin Xu[5]

[1]Laboratory for Climate and Ocean–Atmosphere Studies, Department of Atmospheric and Oceanic Sciences, School of Physics, Peking University, Beijing, 100871, China
[2]Institute of Carbon Neutrality, Peking University, Beijing, 100871, China
[3]Meteorological Observation Center of China Meteorological Administration, Beijing, 100081, China
[4]College of Urban and Environmental Sciences, Peking University, Beijing, 100871, China
[5]Key Laboratory for Atmospheric Chemistry, Institute of Atmospheric Composition, Chinese Academy of Meteorological Sciences, Beijing, 100081, China

Correspondence to: Jintai Lin (linjt@pku.edu.cn)

Abstract. Changes in tropospheric ozone over the Tibetan Plateau (TP) profoundly affect the local ecosystems and human health. Yet previous studies on the TP ozone have focused on the background regions, with much less attention on the urban ozone. Here we quantify the ozone trends over the whole TP from 2015 to 2019 in the context of its long-term trends, with a focus on urban ozone. For this purpose, we use ozone measurements from 30 urban stations in 17 cities from the Ministry of Ecology and Environment (MEE) of China, the Waliguan baseline station, and four satellite products of tropospheric ozone. We further analyze the drivers of ozone trends through a combination of chemical transport model simulations, back-trajectory calculations, a bottom-up emission inventory, and a recent satellite-derived emission dataset of nitrogen oxides (NO_x). We find a strong increase in deseasonalized urban ozone at the MEE stations from 2015 to 2019 (by 1.71 ppb yr^{-1}), which continues after the COVID-19 shock in 2020. The urban ozone trend far exceeds the trend at Waliguan (by 0.26 ppb yr^{-1}) and the TP average trend (by up to 0.08 ppb yr^{-1}) derived from the four satellite products. Interannual variations in meteorology do not produce significant ozone trends over the TP. Non-local factors contribute positively to the urban ozone trends, due mainly to more frequent transport passing through the footprint layers (0–300 m above the ground) of non-local high-emission regions. Another important contributor to the urban ozone growth is the 26.5% increase in local anthropogenic NO_x emissions. Emission reductions in both the local and non-local source regions can help mitigate the rapid urban ozone growth over the plateau.

1 Introduction

Tropospheric ozone is an important pollutant affecting human and ecosystem health (Atkinson et al., 2013; Desqueyroux et al., 2002; Mauzerall and Wang, 2001). Ozone is also a potent greenhouse gas and the main source of the hydroxyl radical (OH, the leading atmospheric oxidant) (Wang et al., 2019; Warneck, 1999). In recent years, surface ozone over eastern and southern China, such as Beijing-Tianjin-Hebei, Yangtze River Delta and Pearl River Delta, have experienced rapid increases.

https://doi.org/10.5194/egusphere-2024-3471
Preprint. Discussion started: 25 November 2024

Numerous studies have analyzed the roles of local human activities, chemistry, meteorology and atmospheric transport in the exacerbation of ozone pollution over these regions (Li et al., 2021; Liu et al., 2023a; Tan et al., 2023).

The Tibetan Plateau (TP; 27–45° N, 70–105° E; Fig. 1), located in southwestern China, covers about 2.5 million km^2 and has an average altitude of more than 4000 m. Most of the Chinese part of the plateau is occupied by Qinghai Province in the north and Tibet in the south. The TP consists mainly of natural wetlands and alpine forests, with few populations and industries, which makes the region an important area to study Asian background ozone. Along with the recent economic development, the gross domestic product (GDP) of Qinghai and Tibet increased by 46% and 63% from 2015 to 2019 (National Bureau of Statistics of China, https://www.stats.gov.cn/, last accessed on June 3, 2024). Industrial and economic development may lead to increased emissions of ozone precursors such as NO_x, and it has been shown that NO_x ozone production efficiency is higher at high altitudes, with the same amount of NO_x emitted potentially leading to more ozone production (Wang et al., 2018). Thus, the ozone changes over the TP urban areas are becoming increasingly important.

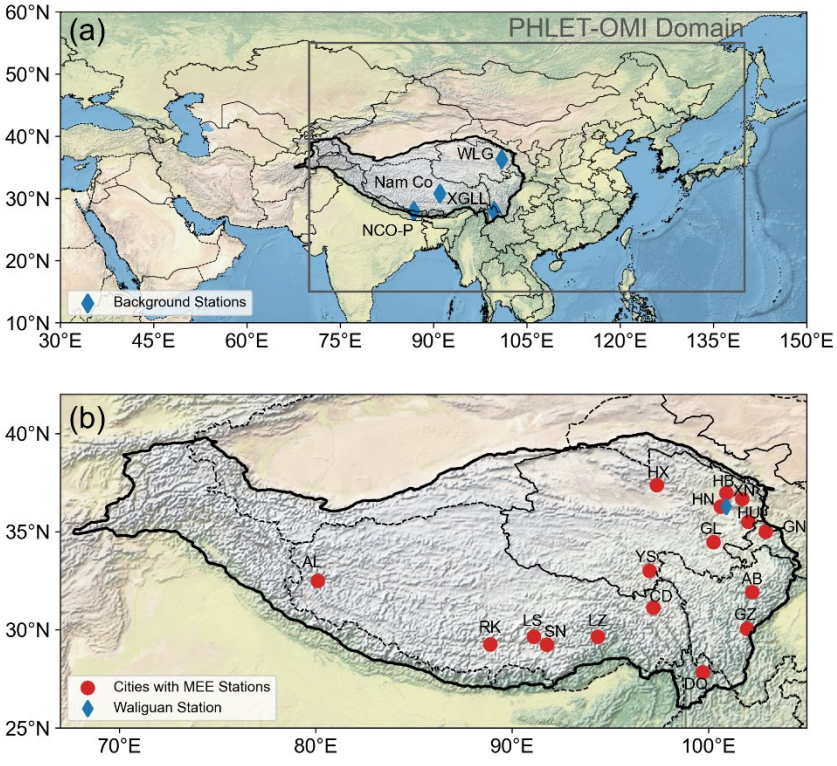

Figure 1 (a) The domain of PHLET-OMI NO_x emission data. The blue diamonds denote the background stations on the TP, including the Nepal Climate Observatory-Pyramid station (NCO-P), the Nam Co Comprehensive Observation and Research Station (Nam Co), Mt.Waliguan Global Atmospheric Watch Station (WLG) and the Xianggelila Regional Atmosphere Background Station (XGLL). (b) Distribution of ground stations used in the study (made with Natural Earth), together with

https://doi.org/10.5194/egusphere-2024-3471
Preprint. Discussion started: 25 November 2024

administrative (dashed line) and TP boundaries (solid line). The TP boundaries are downloaded from the Integration dataset of Tibet Plateau boundary (https://data.tpdc.ac.cn/zh-hans/data/61701a2b-31e5-41bf-b0a3-607c2a9bd3b3/, last accessed on June 3, 2024). The red dots denote the locations of the cities that have MEE stations, including Aba (AB, 3 stations), Ali (AL, 1 station), Changdu (CD, 2 stations), Diqing (DQ, 1 station), Gannan (GN, 1 station), Ganzi (GZ, 1 station), Guoluo (GL, 1 station), Haibei (HB, 1 station), Hainan (HN, 1 station), Haixi (HX, 1 station), Huangnan (HU, 1 station), Lhasa (LS, 6 stations), Linzhi (LZ, 2 stations), Rikaze (RK, 2 stations), Shannan (SN, 2 stations), Xining (XN, 3 stations), Yushu (YS, 1 station).

Previous studies on the TP ozone have mainly concentrated on a small number of background stations near the edges of the plateau, including Waliguan, Xianggelila, Nam Co and Nepal Pyramid (Cristofanelli et al., 2010), or at very high altitude (Zhu et al., 2006). Only a few studies dealt with ozone at TP urban or suburban sites (Ran et al., 2014; Lin et al., 2015b; Chen et al., 2022b). Studies of surface ozone at Waliguan have shown significant growth over the last two decades (Xu et al., 2020), due to atmospheric transport and local emissions (Xu et al., 2016; Xu et al., 2018a). Transport plays important roles at these background stations, but the pollutant source areas are largely station dependent. Ozone at Waliguan in the northern TP is strongly influenced by air masses from northwestern and central China (Xue et al., 2011), Xianggelila on the southeastern TP is mainly influenced by western China and Southeast Asia (Ma et al., 2014), while Nam Co is mainly affected by South Asia (Yin et al., 2017; Xu et al., 2018b). In addition, the Xianggelila and Nepal Pyramid stations are strongly influenced by the South Asian monsoon (Marinoni et al., 2013; Putero et al., 2014; Ma et al., 2014). Such spatial diversity in ozone sources means that more data are needed to study the ozone trends over the entire plateau.

In contrast, only a few studies have used data at the urban stations from the Ministry of Ecology and Environment (MEE) to analyze the TP ozone characteristics. Chen et al. (2022c) used a Geodetector analysis to find that natural factors dominate the urban surface ozone variations over the TP, while the ecological degradation and desertification might have contributed to the ozone growth. Yin et al. (2022) used a random forest model to estimate the contribution of meteorology to surface ozone changes at 12 MEE cities on the TP from 2015 to 2020. Using a variety of meteorological parameters (wind, temperature, pressure, etc.) as predictors, they found that meteorology contributes less than 5% of the interannual variability of ozone at the MEE stations. Overall, the trends and drivers of the TP urban ozone remain understudied.

Several types of numerical methods exist to study the drivers of surface ozone changes, including chemical transport models (CTMs), back-trajectory models, statistical analysis, and machine learning. The CTMs can quantitatively separate the contributions of individual drivers, as have been widely used in the study of Chinese ozone pollution (Ni et al., 2018; Ni et al., 2024; Wang et al., 2024). The CTMs rely on emission inventories for source attribution and are subject to large emission uncertainty for the TP. Chen et al. (2022a) simulated several air pollutants in the TP using WRF-Chem and found substantial underestimation in the modeled pollutant concentrations. They hypothesized that the emission inventory underestimates pollutant emissions on the TP by an order of magnitude. By comparison, the back-trajectory models analyze the transport pathways of air masses, as often used in the TP ozone studies (Chen et al., 2022b; Yang et al., 2022); but these models cannot quantitatively determine the exact locations of ozone formation and precursor emissions. The statistical and machine

https://doi.org/10.5194/egusphere-2024-3471
Preprint. Discussion started: 25 November 2024

learning methods try to correlate ozone concentrations with multiple predicting variables (Weng et al., 2022; Xu et al., 2023; Zheng et al., 2023). For example, the random forest analysis by Yin et al. (2022) suggested the international variations of ozone at the TP MEE stations to be caused by anthropogenic influences, by only quantifying the meteorological impacts with no explicit analysis of atmospheric transport.

Here, we combine multiple observational datasets, emission data and modelling approaches to assess the TP ozone trends and their drivers, with a particular focus on the urban areas where the MEE stations are located. We focus on the ozone trends over 2015–2019 in the context of its long-term changes. We use four satellite products of tropospheric ozone, urban ozone measurements at 30 MEE stations, and background ozone measurements at the Waliguan station to obtain comprehensive information on the ozone changes over the plateau. We then use the GEOS-Chem CTM, the HYSPLIT back-trajectory model, the CEDS bottom-up emission inventory, and a satellite-based top-down emission dataset (PHLET-OMI) of NO_x (nitrogen oxides) to separate the roles of local contribution, non-local contribution and meteorology in the ozone trends. Section 2 presents the ozone datasets, emission datasets, and the configurations of HYSPLIT and GEOS-Chem. Section 3 analyzes the ozone trends. Section 4 quantifies the contributions of individual drivers. Section 5 summarizes the study.

2 Data and methods

2.1 Ground-based near-surface ozone data

Hourly concentrations of surface ozone are taken from the MEE website (http://www.cnemc.cn/en/, last accessed on April 21, 2024). In 2013, a monitoring network for near-surface air pollutant concentrations was launched by the MEE (Li et al., 2019). So far, more than 1500 stations have been established, mostly in the urban areas of China, providing hourly concentrations of six air pollutants including O_3 (ozone), $PM_{2.5}$, PM_{10} (fine particulate matter smaller than 2.5 μm and 10 μm in aerodynamic diameter, respectively), NO_x, SO_2 (sulfur dioxide), and CO (carbon monoxide). These measurement data have been widely used to study the changes and drivers of ozone pollution over central, eastern, and northern China (Liu and Wang, 2020a, b; Lu et al., 2020; Li et al., 2021; Pan et al., 2023; Wang et al., 2024). Between 2013 and 2015, a total of 37 air quality stations in 19 cities of the TP were added into the MEE network.

We apply the quality control method by Lu et al. (2018) to remove unreliable hourly data from the MEE stations, and use the method by Yan et al. (2018a) to obtain city-averaged, daily-averaged, and monthly-averaged ozone mixing ratios. First, stations with more than 30% of hourly data missing during 2015–2019 are removed. For a given city, city-level hourly data are obtained by averaging all the selected stations in this city (Fig. 1). Then we discard the days with more than 30% of hourly data missing. Finally, we discard any months with valid data less than 20 days. After quality control, 30 stations in 17 cities are selected. Figure 1 shows the locations of these cities.

Ozone mixing ratios at the Waliguan station (36.28° N, 100.90° E) from 1994 to 2016 are obtained from the TOAR website (Tropospheric Ozone Assessment Report, https://igacproject.org/activities/TOAR, last accessed on April 21, 2024). Monthly

https://doi.org/10.5194/egusphere-2024-3471
Preprint. Discussion started: 25 November 2024

average ozone mixing ratios at the Waliguan station from 2017 to 2019 are calculated by the Meteorological Observation Centre of the China Meteorological Administration. These data have been utilized extensively to study the background ozone (Xu et al., 2018a; Xu et al., 2020; Han et al., 2023; Ye et al., 2024). TOAR also includes the Xianggelila station (28.01° N, 99.44° E) and Nepal Pyramid station (27.95° N, 86.82° E) for hourly ozone concentrations. However, data from Xianggelila and Nepal Pyramid are only available through 2016 and 2014, respectively. In addition, these two stations are located on the southern edge of the TP and are significantly influenced by the South Asian monsoon (Ma et al., 2014; Cristofanelli et al., 2010), making them difficult to represent the ozone characteristics over the vast area of inner TP. There is also a Nam Co station on the south-central TP, but data from this station are not available. Thus, these three stations are not included in this study.

The ozone time series includes substantial seasonality due to seasonal variations in natural conditions and anthropogenic activities (Kalsoom et al., 2021). To uncover the ozone trend, we subtract the multi-year averaged seasonality from the monthly mean time series to obtain a deseasonalized dataset.

2.2 Satellite-based tropospheric ozone data

We use four satellite-based level-3 monthly tropospheric column ozone (TCO) products to analyze the tropospheric ozone changes over the entire TP. The first product is the OMI/MLS (Ozone Monitoring Instrument/Microwave Limb Sounder, https://acd-ext.gsfc.nasa.gov/Data_services/cloud_slice/new_data.html, last accessed on April 21, 2024). This product is calculated by subtracting the MLS stratospheric column ozone from the OMI total column ozone, with a horizontal resolution of 1° lat. × 1.25° long. covering the areas from 60° S to 60° N. Data are available since 2014. Ziemke et al. (2011) showed that the OMI/MLS data are in good correlation with ozonesonde measurements, with correlation coefficients ranging from 0.8 to 0.9 for the years 2005–2008 for WOUDC (World Ozone and Ultraviolet radiation Data Center) ozonesondes and 2004–2009 for SHADOZ (Southern Hemisphere Additional Ozonseondes) ozonesondes. The OMI/MLS TCO is lower than the ozonesonde data by about 1 ppb on average. OMI/MLS also shows good agreement with CTM simulation results (Ziemke et al., 2006; Yan et al., 2016). The second satellite product used here, OMI-RAL, is based on an optimal estimation method (OEM, Miles et al. (2015)) and has been updated by the Copernicus Climate Change Service (C3S, https://cds.climate.copernicus.eu/cdsapp#!/dataset/satellite-ozone?tab=form, last accessed on April 21, 2024). In deriving OMI-RAL, the ozone vertical profiles from the ground to 450 hPa are produced based on the strongly variable ozone absorption at 280–320 nm. OMI-RAL spans from October 2004 to the present with a horizontal resolution of 1° × 1°.

The third product, IASI-FORLI, provides global ozone column data from the surface to 6 km above sea level at 1° × 1° from January 2008 to the present (https://cds.climate.copernicus.eu/cdsapp#!/dataset/satellite-ozone?tab=form, last accessed on April 21, 2024). The product is retrieved with the FORLI-O_3 OEM (Boynard et al., 2016). Boynard et al. (2018) showed that the IASI-FORLI tropospheric column is slightly higher than ozonesonde data in the high latitudes (by 4 %–5 %) and lower in the midlatitudes and tropics (by 11 %–13 % and 16 %–19 %, respectively). The fourth product, IASI-SOFRID, provides global tropospheric columns and profiles of ozone at 1° × 1° since January 2008 (https://thredds.sedoo.fr/iasi-sofrid-o3-co/,

https://doi.org/10.5194/egusphere-2024-3471
Preprint. Discussion started: 25 November 2024

last accessed on April 21, 2024). The product is retrieved by SOFRID OEM, which is built based on the RTTOV (Radiative Transfer for TOVS) operational radiative transfer model (Matricardi et al., 2004). Good correlation (0.82) exists between IASI-SOFRID and ozonesonde data in 2008 in the midlatitudes (Dufour et al., 2012).

However, Boynard et al. (2018) found a negative drift in the IASI level-2 data, which leads to a negative drift of -8.6±3.4% decade^{-1} in IASI-SOFRID for the Northern Hemisphere comparing with the ozonesonde data. IASI-FORLI also shows a negative drift of -3.0% decade^{-1} for 0–60°N (Barret et al., 2020). Therefore, we correct the ISAI-SOFRID and IASI-FORLI ozone data by subtracting the drift trends above to the original ozone data.

For comparison with ground-based ozone measurements, tropospheric column ozone concentrations from the satellite products are converted to tropospheric mean mixing ratios. Following Ziemke et al. (2001), the concentration conversion employs the ideal gas equation of state, assuming hydrostatic equilibrium and constant gravity in the troposphere. Note that OMI/MLS and IASI-SOFRID ozone data represent the total tropospheric ozone column, OMI-RAL represents the ozone column from the ground to 450 hPa, and IASI-FORLI represents the ozone column from the ground to 6 km above sea level. As such, the converted ozone mixing ratios represent different vertical extents. In addition, all satellite data are de-seasonalized prior to the trend analysis, as done for the ground-based ozone measurements.

2.3 Model simulations

We use the HYSPLIT (Hybrid Single-Particle Lagrangian Integrated Trajectory) model to calculate the back-trajectories of a large number of particles (Cohen et al., 2015) affecting Waliguan and the 17 cities with MEE measurements. To drive the model, we use the MERRA2 assimilated meteorological data (GMAO, 2015a, b, c, d). The MERRA2 data have a horizontal resolution of 0.5° lat. × 0.625° long. and 72 vertical levels, with each of the lowest 10 layers about 130 m thick. Particles are transported by the average winds and a turbulence transport component. The Kantha-Clayson scheme is adopted to compute the vertical turbulence (Kantha and Clayson, 2012).

We calculate the back-trajectories to quantify the transport of anthropogenic pollutants, following previous work (Stohl, 2003; Cooper et al., 2010; Ding et al., 2013). For each city and Waliguan, an amount of 2000 particles are released from 100 m above the ground for each hour from 1 January 2015 to 31 December 2019, and the total run time for each particle is 192 h backward. In total, we conduct 1.6 billion back-trajectories for 17 cities and Waliguan in this study. The residence time distribution of the air mass is output as monthly averages on a 0.5° × 0.5° grid. Then the "retroplume" is obtained with a unit of s kg^{-1} m^3, which represents the residence time of a simulated air mass divided by the air density. The residence time of the back-trajectory particles passing through the footprint layer (0 to 300 m above ground) can be multiplied by NO_x emissions (into the footprint layer, in units of kg m^{-3} s^{-1}) to calculate the quantity emitted into the retroplume (QNR, as mixing ratio) for NO_x. As such, the QNR can roughly characterize the strength of ozone transport from individual emission source regions (Cooper et al., 2010; Stohl, 2003). The QNR does not consider the nonlinearity in ozone formation chemistry, which may introduce certain uncertainty.

https://doi.org/10.5194/egusphere-2024-3471
Preprint. Discussion started: 25 November 2024

To evaluate the role of meteorological changes from 2015 to 2019, we use the GEOS-Chem CTM (v13.3.3; https://geoschem.github.io/, last access: 10 April 2024). In general, it is difficult for a CTM to simulate the urban pollution over the TP (Chen et al. (2022a)), due to inadequacies and inaccuracies in the representation of complex terrains, fine-scale chemistry and precursor emissions. Thus, we only use GEOS-Chem to quantify the effect of large-scale meteorological changes on ozone. The model is driven by MERRA2 at 2° lat. × 2.5° long. with 72 vertical layers. It computes the convective transport of chemicals from the archived MERRA2 convective mass fluxes (Wu et al., 2007). A non-local scheme for vertical mixing within the planetary boundary layer is implemented to account for different states of mixing based on the static instability (Lin and Mcelroy, 2010). For anthropogenic emissions, we use the MEIC (Multi-scale Emissions Inventory of China; www.meicmodel.org) inventory in China (Li et al., 2017; Zheng et al., 2018) and the CEDS (Community Emissions Data System v_2021_02_05) inventory in other regions (O'rourke, 2021). For soil NO_x, sea salt aerosols, and biogenic volatile organic compounds, we use an offline dataset at a horizontal resolution of 0.25° lat. × 0.3125° long. (Weng et al., 2020). The GEOS-Chem model is run with anthropogenic emissions fixed at the 2015 levels while allowing the meteorology and meteorology-driven natural emissions to vary with time. The simulation period is from October 2014 to December 2019, with the first three months used for spin-up to reduce the effect of initial conditions.

2.4 Anthropogenic emission data for NO_x

In the TP region, the bottom-up anthropogenic emission inventories contain large uncertainties due to inaccuracy and inadequacy in human activity statistics and emission factors (Geng et al., 2017; Chen et al., 2022a). Thus, for the back-trajectory calculations, we use top-down NO_x emission data to reduce the effect of emission errors. The top-down NO_x emission data are from PHLET-OMI (Kong et al., 2022; Kong et al., 2019), which estimates June–August average NO_x emissions at 0.05° × 0.05° in Asia (15°-55° N, 70°-140° E; Fig. 1a). PHLET-OMI is obtained by employing the POMINO-OMI satellite product for tropospheric NO_2 vertical column densities (VCDs) (Liu et al., 2019; Lin et al., 2015a; Lin et al., 2014) and the PHLET algorithm for emission retrieval. The PHLET emission data reveal considerable amounts of emission sources unaccounted in existing bottom-up anthropogenic emission inventories (Kong et al., 2022) and natural emission parametrization (Kong et al., 2023). For example, the provincial total anthropogenic emissions of Tibet in PHLET are higher than current inventories by 3 to 7 times (Kong et al., 2022). PHLET-OMI provides June–August average NO_x emissions in each year from 2012 to 2020. We remove the contributions of natural emission sources to focus on anthropogenic influences, following the method by Kong et al. (2022).

To make use of the PHLET-OMI anthropogenic NO_x emissions within its spatial domain and account for the monthly variation in emissions, we combine PHLET-OMI with the monthly variation from the CEDS inventory (Eq. (1)):

$$E^{adjust}_{r,g,y,m} = E^{PHLET}_{r,g,y} \frac{E^{CEDS}_{r,g,y,m}}{\sum_{m=6}^{8} n_m E^{CEDS}_{r,g,y,m} / \sum_{m=6}^{8} n_m}, \quad (1)$$

https://doi.org/10.5194/egusphere-2024-3471
Preprint. Discussion started: 25 November 2024

where r represents a region (a province in China or a country in the rest of Asia), g represents a grid cell within the region r, y represents a year, and m represents a month. n_m represents the number of days in the month m. For regions outside the PHLET-OMI domain, the CEDS inventory is used directly.

3 Elevated ozone concentrations

Figure 2 compares the monthly variation of deseasonalized ozone concentrations at Waliguan and 17 cities with MEE measurements. The MEE stations are located in the urban areas with local anthropogenic influences. In contrast, the Waliguan station is situated on the Waliguan Mountain with few local anthropogenic emissions, and thus its ozone concentrations are mainly influenced by the free troposphere, stratosphere and the global background ozone (Xu et al., 2018a; Xu et al., 2020). We use linear regression to derive ozone trends.

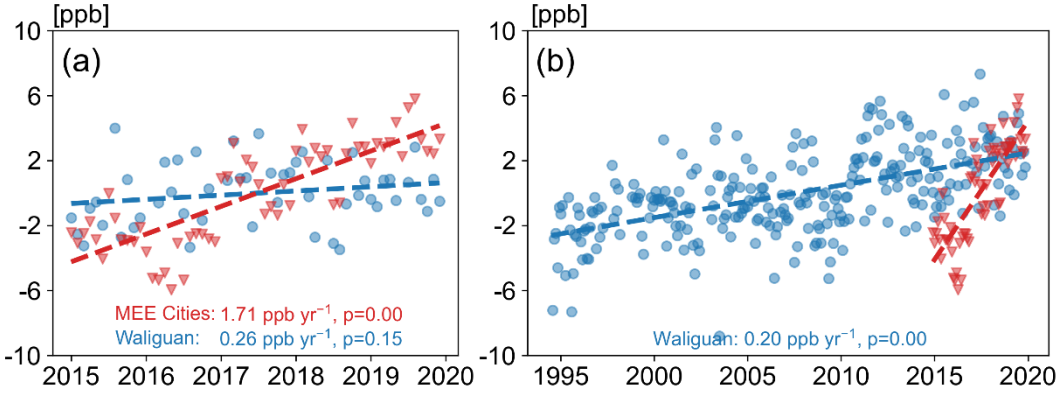

Figure 2. Monthly variation of deseasonalized ozone mixing ratios over the TP during (a) January 2015 to December 2019 and (b) August 1994 to December 2019 based on ground measurements. The results of MEE cities represent the mean of ozone mixing ratios in 17 cities. The data points represent deseasonalized ozone in individual months, and the dashed lines represent linear regression fit. The slope of linear regression and the p-value are also shown.

Deseasonalized ozone mixing ratios at Waliguan increase at a rate of 0.26 ppb yr^{-1} from 2015 to 2019 (Fig. 2a), which is consistent with the long-term trend from October 1994 to December 2019 (Fig. 2b). By comparison, deseasonalized ozone mixing ratios at the MEE stations averaged over 17 cities show much stronger growth (1.71 ppb yr^{-1}) during 2015–2019, suggesting potential influences from local human activities. The MEE ozone declines from 2019 to 2020, likely due to COVID-19, but it resumes rapid growth in the following years (by 1.89 ppb yr^{-1}) until the second half of 2023 (Fig. S1). Overall, the trend of MEE ozone over 2015–2019 represents the growth during the most recent decade. This general growth is in contrast to the ozone changes over the North China Plain and Yangtze River Delta region, which show a rapid rise from 2013 to 2017 and a leveling off after 2017 (Liu et al., 2023b). Such contrast likely reflects the regional differences in

https://doi.org/10.5194/egusphere-2024-3471
Preprint. Discussion started: 25 November 2024

emission regulation. The central and eastern regions of China have had stringent emission reduction requirements, whereas the western regions are the most lenient in emission regulation (CSC, 2016). The regional difference in environmental regulation could also lead to more polluting factories moving to western China, making it more difficult to reduce emissions there (Cui et al., 2016; Zhao et al., 2017; Zheng and Shi, 2017).

To examine whether the TP ozone trends exhibit strong dependence on the time of day, we further explore the MEE measurements. The MEE ozone at different hours in the daytime show similar strong growth from 2015 to 2019 (Fig. S2). Ozone increases at a rate of 2.15 ppb yr^{-1} in the early afternoon (local solar time (LST) 13:00, close to the overpass time of OMI), at a rate of 1.60 ppb yr^{-1} in the morning (LST 09:00, close to the overpass time of IASI), and at a rate of 1.86 ppb yr^{-1} for the maximum daily 8-hour average (MDA8).

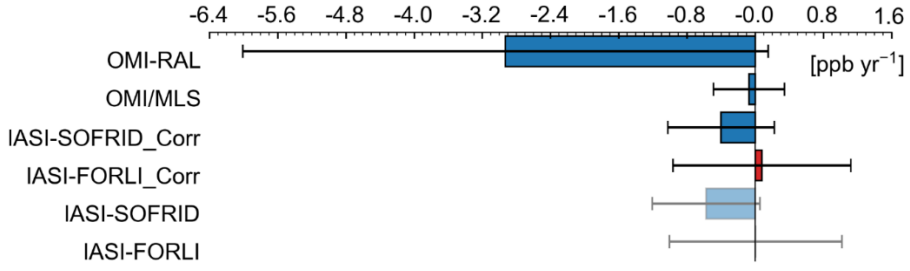

Figure 3 Trends of deseasonalized tropospheric ozone mixing ratios from 2015 to 2019 based on different satellite datasets. The error bar represents the standard deviation of all gridded data over the TP. The '_Corr' suffix means that the data have been corrected, as described in Section 2.3.

The TP is a vast area, and its ozone characteristics may vary considerably across the plateau (Yin et al., 2017). Therefore, we further examine four satellite products of tropospheric ozone to assess the ozone changes over the whole plateau (Fig. 3). Considering the drift in the IASI ozone data, we analyze the drift-corrected data (IASI-SOFRID_corr and IASI-FORLI_corr), with the original IASI data presented only for record.

From 2015 to 2019, OMI-RAL shows a strong ozone decline over 2015–2019 when averaged over the plateau, whereas other products suggest weak plateau-average ozone trends (within ±0.3 ppb yr^{-1}) (Fig. 3). This is different from the long-term trends in these four products, which show growth over 2008–2019 (Fig. S3). Spatially (Fig. 4), OMI-RAL suggests strong ozone decline at most places, but with sporadic positive trends. OMI/MLS, IASI-SOFRID_Corr and IASI-FORLI_Corr suggest slight ozone decline over the southern plateau and growth over the northern plateau, although the magnitudes of ozone trends are within ±0.5 ppb yr^{-1}.The spatial distributions of ozone trends over 2015–2019 are also different from the long-term growing trends over 2008–2019 in these four products (Fig. S4). The reasons for the inconsistent results of these satellite data are complex and may be related to their different observing equipments, different methods of inversion from

https://doi.org/10.5194/egusphere-2024-3471
Preprint. Discussion started: 25 November 2024

radiance spectra to tropospheric ozone abundance, different retrieval altitudes, and different overpass times. Nevertheless, none of the satellite products shows ozone growth between 2015 and 2019 at a magnitude similar to that at the MEE stations.

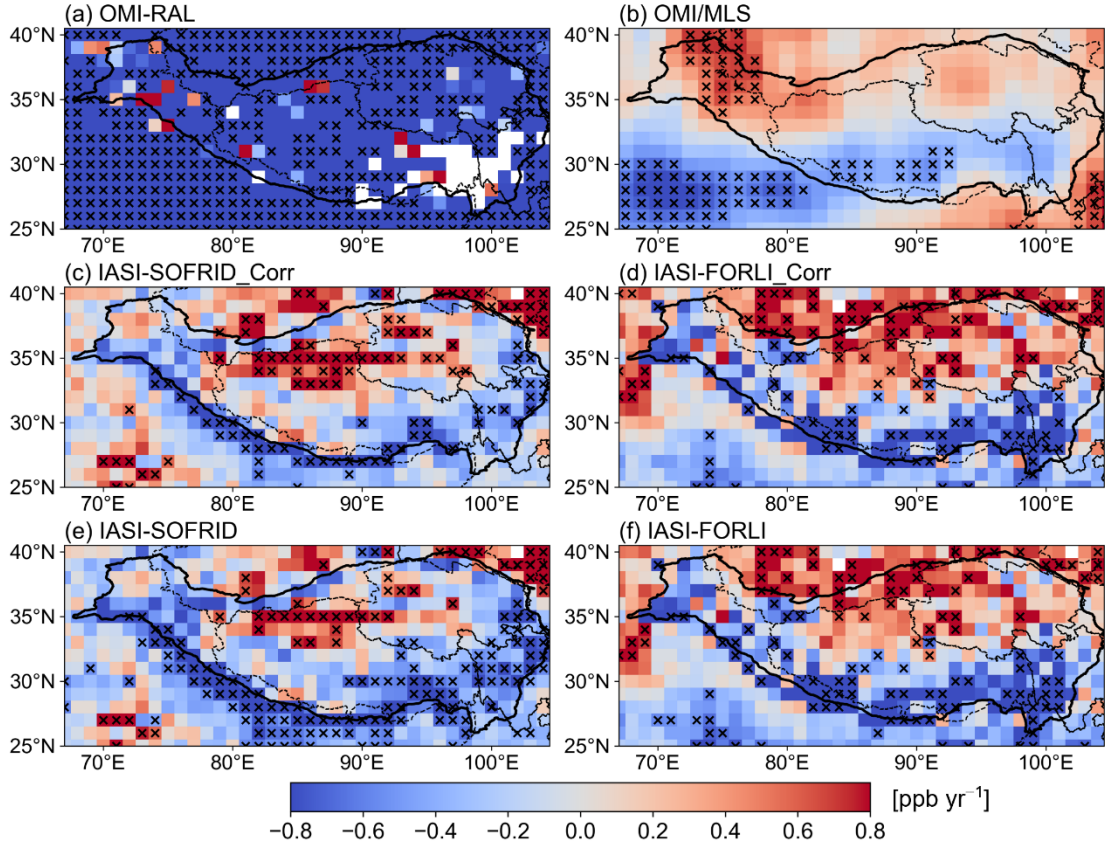

Figure 4 Spatial distribution of deseasonalized tropospheric ozone mixing ratio trends from 2015 to 2019 for (a) OMI-RAL, (b) OMI/MLS, (c) IASI-SOFRID_Corr, (d) IASI-FORLI_Corr, (e) IASI-SOFRID, and (f) IASI-FORLI. Each cross means the trend in that grid cell is statistically significant (p-value < 0.05).

In summary, the MEE data exhibit strong ozone growth from 2015 to 2019, in contrast to the much weaker ozone changes shown in the Waliguan background station and satellite datasets.

4 Drivers of ozone trends

Near-surface ozone concentrations are influenced by meteorological conditions and local emissions (Lu et al., 2019; Yan et al., 2018a; Yan et al., 2018b). Over the TP, atmospheric transport of ozone and precursors from non-local source regions is

https://doi.org/10.5194/egusphere-2024-3471
Preprint. Discussion started: 25 November 2024

also an important factor (Xu et al., 2016; Ma et al., 2014). In particular, regional transport from Asian countries has a strong influence on the tropospheric ozone over the plateau (Ni et al., 2018; Ma et al., 2022; Hu et al., 2024).

In this section, we analyze the individual contributions of three factors to the ozone changes over the TP, including meteorology, non-local contributor and local contributor. For simplicity, we only analyze the drivers of trends in daily average ozone. Here, the "meteorology" represents the combined effect of meteorological changes (captured by GEOS-Chem simulations at 2° lat. × 2.5° long.), meteorology-induced natural emission changes and stratosphere-troposphere exchange that affects the global background ozone. The "non-local contributor" represents the combined effect of changes in precursor emissions and air mass transport pathway over the areas within 192 hours of back-trajectory but outside the 1.5° latitude-longitude range of a receptor (the average location of MEE stations within a city or the location of Waliguan background station). The choice of the 1.5° range is made after considering the pixel size and data availability of OMI NO_2 product (Lin et al., 2015a; Zhang et al., 2022) which is used to derive PHLET-OMI NO_x emissions (Kong et al., 2019; Kong et al., 2022; Kong et al., 2023). The "local contributor" refers to the combined effect of anthropogenic emissions and transport pathway over the areas inside the 1.5° range of the receptor. The transport pathway affects the amount of residence time the air mass is situated in the footprint layers of high-emission regions.

4.1 Effect of meteorology

Figure 5 shows the effect of changes in meteorology on surface ozone over the TP during 2015–2019, as simulated by GEOS-Chem at 2° lat. × 2.5° long. with fixed anthropogenic emissions but temporally varying meteorology. Over the plateau, ozone mixing ratios change little, except for the slight growth over the western and southeastern plateau and decline along the southern edge (Fig. 5b). The plateau-average rate of change is only about -0.08±0.2 ppb yr^{-1}. At the Waliguan station and the 17 cities with MEE data, the rates of change are -0.15ppb yr^{-1} and -0.1±0.16 ppb yr^{-1}, respectively. Thus meteorology is not an important factor for the observed ozone growth of 1.71 ppb yr^{-1} at the MEE stations (Fig. 2). This result is consistent with previous work for 12 cities with MEE stations over the TP based on a random forest model (Yin et al., 2022).

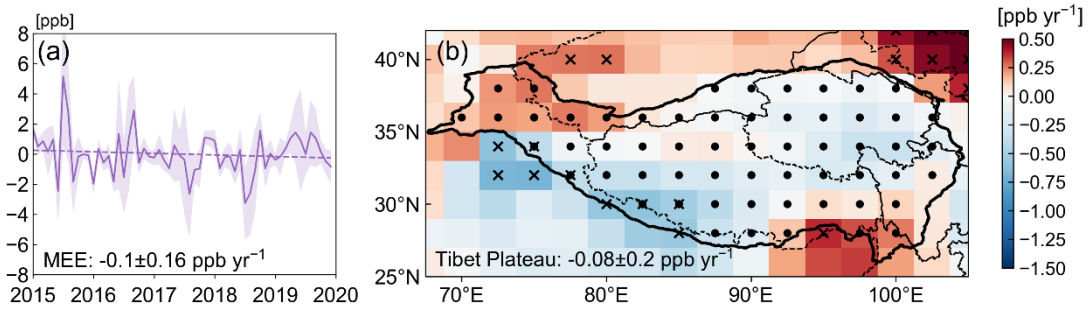

Figure 5 Changes in ozone mixing ratios due to changes in meteorology over 2015–2019 simulated by GEOS-Chem. (a) Deseasonalized monthly mean ozone averaged over the 17 cities with MEE measurements. (b) Spatial distribution of

https://doi.org/10.5194/egusphere-2024-3471
Preprint. Discussion started: 25 November 2024

deseasonalized ozone trends over the plateau. In (b), the dots denote the grid cells belonging to the TP, and the crosses denote statistically significant ozone trends (p-value < 0.05).

4.2 Effect of non-local contributor

To evaluate the effect of non-local contributor, we use the HYSPLIT model to conduct 192-hour back-trajectories for the 17 cities and Waliguan during 2015–2019. We do not use GEOS-Chem simulations here, considering that the large uncertainty in current emission datasets of volatile organic compounds in the TP (Li et al., 2023a; Li et al., 2023b) does not allow reliable high-resolution simulations to capture the urban ozone chemistry.

As shown in Fig. 6, air masses reaching the 17 TP cities with 192 hours come from China and nearly countries. Most air masses reaching the 17 cities stay at the edge of the plateau for a long time, because the air masses are blocked by the topography (e.g., the Himalayas). Among the source areas outside China, Nepal, Northeastern India, Myanmar and Bangladesh exhibit longer residence time in the footprint layer (i.e., 0–300 m above the ground). Overall, there is little interannual variation in the spatial distribution of residence time. In 2018, there was an increase in residence time over the eastern part of China, likely due to more pronounced easterly winds in the lower troposphere on the eastern side of the plateau (not shown). Such wind anomaly is associated with the subtropical high anomaly in summer 2018 (Yuan et al., 2019; Ding et al., 2019). Summer is the high ozone season in eastern China, and the increased residence time of air masses from the east may lead to increased ozone transport.

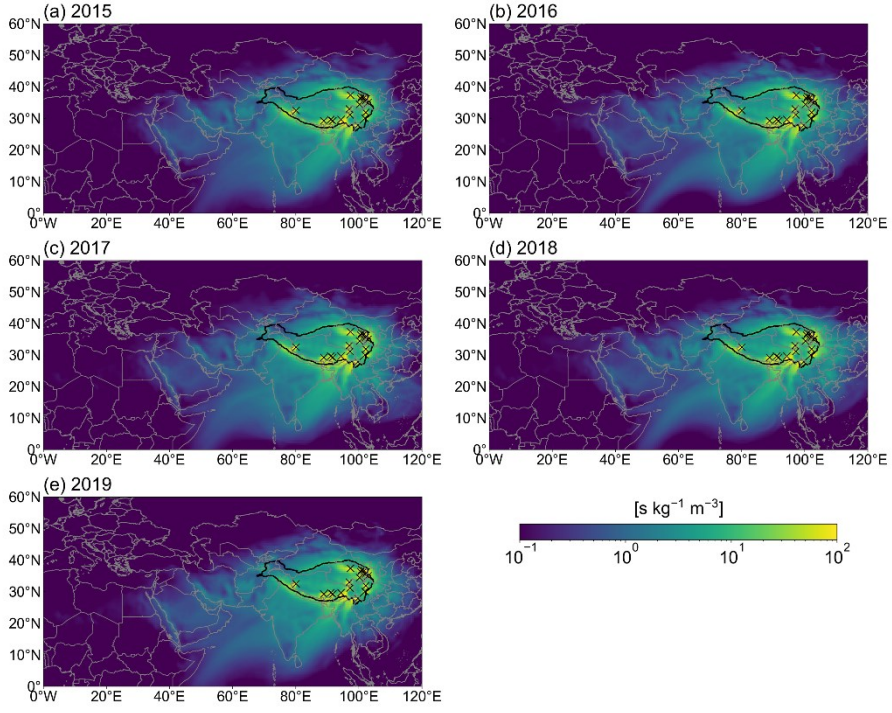

https://doi.org/10.5194/egusphere-2024-3471
Preprint. Discussion started: 25 November 2024

Figure 6 Distribution of the annual average residence time in the footprint layer for the 17 cities with MEE stations in (a) 2015, (b) 2016, (c) 2017, (d) 2018, (e) 2019. The crosses denote the locations of 17 cities.

To further quantify the non-local contribution through transport, we calculate the non-local QNR by multiplying the residence time in the footprint layer of individual locations and their NO_x emissions and then summing over those locations outside the 1.5° range of each receptor. From 2015 to 2019, the non-local QNR increases at a rate of 0.11 ppb yr^{-1} (p-value = 0.19) (Fig. 7a). The QNR growth rate due to changes in transport pathway alone is about 0.10 ppb yr^{-1} (p-value = 0.15), while emission changes alone result in little trend of QNR (Fig. 7b-c). For individual years, summer 2018 exhibits the highest QNR as a result of longer residence time in the footprint layer of high-NO_x eastern China. Meanwhile, emission changes result in high QNR in summer 2017, and both emissions and transport pathway contribute to low QNR values in 2015 and 2019.

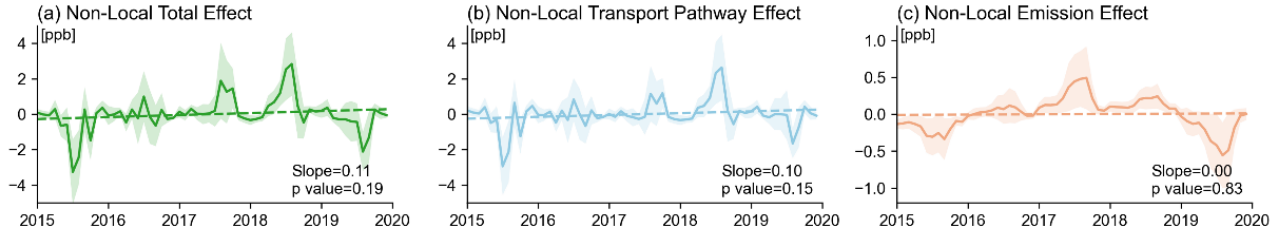

Figure 7 Deseasonalized monthly variation of non-local QNR averaged over the 17 cities. (a) Non-local QNR changes due to the combined effect of changes in anthropogenic emissions and in transport pathway. (b) Non-local QNR changes due to transport pathway alone. (c) Non-local QNR changes due to anthropogenic emissions alone. The shaded area represents the standard deviation of the data across 17 cities.

The interannual variation of QNR for the Waliguan background station is similar to that for the MEE stations (Fig. S5). These results suggest a considerable positive contribution of regional transport to ozone growth over the whole plateau.

4.3 Effect of local contributor

To further delineate the contribution of changes in local air mass residence time and anthropogenic emissions, we analyze the local PHLET-OMI NO_x emissions and QNR for within the 1.5° range of the 17 cities. The interannual variation of three-year summer average local NO_x emissions show a growth of 26.5% from 1.81 tons h^{-1} in 2015 to 2.29 tons h^{-1} in 2019 (Fig. 8a). This suggests an important contribution from local anthropogenic emissions in the elevated urban ozone over the TP.

https://doi.org/10.5194/egusphere-2024-3471
Preprint. Discussion started: 25 November 2024

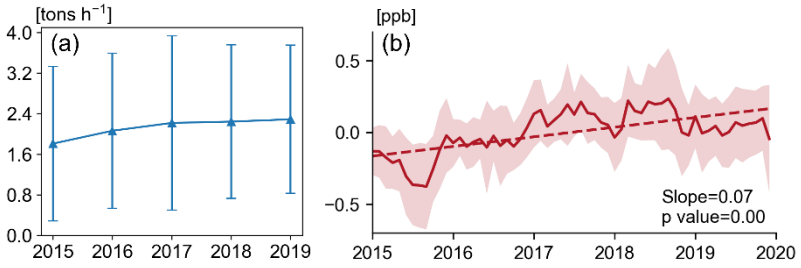

Figure 8 Changes in local anthropogenic emissions and QNR for within 1.5° of the 17 cities. (a) Time series of three-year moving average PHLET-OMI NO_x anthropogenic emissions in summer. Here, the value for 2015 represents the average over 2014–2016, and so on. (b) Deseasonalized monthly variation of local QNR. The error bar in (a) and shaded area in (b) represent the standard deviation of data across 17 cities.

Figure 8b further shows that for the 17 cities, the local contribution to QNR increases significantly from 2015 to 2019 with a trend of 0.07 ppb yr^{-1}, with a total growth of 30% over these years. This trend is contributed mainly by the growth in local NO_x emissions (26.5%). It contrasts with the respective trend of local QNR for Waliguan (-0.07ppb yr^{-1}) (Fig. S5d). The local QNR growth for the 17 cities (0.07 ppb yr^{-1}) is smaller than that for the non-local contribution (0.11 ppb yr^{-1}, Fig. 7a). However, note that the QNR calculation does not consider the effect of distance from the emission source regions to the TP cities and the associated ozone loss (through chemical reactions and/or dry deposition) along the transport pathway. Taking the distance into account, each unit of ozone mass produced from more distant source regions might be lost more substantially and thus have a weaker effect on these cities. This means that the local contribution is indeed a major cause of ozone growth in the 17 cities.

A simplified linear model can be established to delineate the contributions to ozone change at the TP cities from the three factors (meteorology, the non-local QNR, and the local QNR):

$$T_{total} = T_{met} + aQ_{nonlocal} + bQ_{local}, \quad (2)$$

where T_{total} is the total ozone trend, T_{met} is the ozone trend due to meteorology, and $Q_{nonlocal}$ and Q_{local} represent the trends of QNR for the non-local and local contributors, respectively. The coefficients a and b can be regarded as a combination of ozone production efficiency in converting NO_x to ozone and ozone loss during transport. For the cities, T_{total}, T_{met}, $Q_{nonlocal}$ and Q_{local} are 1.71 ppb yr^{-1}, -0.10 ppb yr^{-1}, 0.11 ppb yr^{-1} and 0.07 ppb yr^{-1}, respectively. For Waliguan, T_{total}, T_{met}, $Q_{nonlocal}$ and Q_{local} are 0.26 ppb yr^{-1}, -0.15 ppb yr^{-1}, 0.18 ppb yr^{-1} and -0.07 ppb yr^{-1}. Combining these T and Q values yields an estimate of a at 7.7 and b at 13.8. This result means that the change in each unit of QNR from local factors has a much higher impact on ozone than the QNR for the non-local factors, due to a higher ozone production efficiency and/or less ozone loss.

https://doi.org/10.5194/egusphere-2024-3471
Preprint. Discussion started: 25 November 2024

5 Conclusions

This study uses the ozone measurements from MEE, Waliguan and satellite products to analyze the ozone changes over the TP. The ozone mixing ratios at the MEE stations in the urban areas increases significantly at a rate of 1.71 ppb yr^{-1} from 2015 to 2019 averaged over 17 cities. A similar rate of growth occurs after the plateau resumes from the COVID-19 shock in 2020. In contrast, ozone at Waliguan rises at a rate of 0.26 ppb yr^{-1} from 2015 to 2019, consistent with its long-term trend over 2008–2019. Additionally, tropospheric ozone over the TP does not suggest a strong upward trend from 2015 to 2019. These results suggest strong anthropogenic influences on ozone growth over the TP cities over the past decade.

We further quantify the contributions of three factors to the ozone growth at the cities by using GEOS-Chem simulations, HYSPLIT calculations, the CEDS emission inventory and the PHLET-OMI top-down emission dataset. These factors include meteorology, local contributor and non-local contributor. As simulated by GEOS-Chem, the meteorological changes over the plateau do not result in near-surface ozone growth between 2015 and 2019, albeit with clear interannual variations. The meteorology-driven ozone trends over the whole TP and the 17 cities are only -0.10 ± 0.16 ppb yr^{-1} and -0.08 ± 0.20 ppb yr^{-1}, respectively.

In contrast, the non-local QNR, calculated by combining the HYSPLIT modeling and NO_x emissions for the areas outside 1.5° range of each city, exhibits a growth rate of 0.11 ppb yr^{-1}. This suggests a substantial non-local contribution to the urban ozone trends. The non-local contribution is due mainly to the changes in transport pathway of air mass rather than the changes in anthropogenic emissions. This means that the growth of urban ozone over the TP may be related to more frequent transport of air masses passing through non-local high-emission regions.

The local QNR for the 17 cities exhibits a growth of 0.07 ppb yr^{-1} (or 30% in total) from 2015 and 2019, with the majority caused by the increase in local NO_x emissions (by 26.5%). Considering the ozone loss during atmospheric transport at different distances, local and non-local contributions to the rapid rise in the TP urban ozone might be comparable. This is further supported by a simple linear model showing that on a per unit basis, the contribution of local QNR to the urban ozone growth is much larger than that of non-local QNR (13.8 versus 7.7).

Overall, our study suggests that the large rate of urban ozone growth over the TP cities during the recent decade is caused mainly by a combination of increases in local anthropogenic emissions and more frequent transport passing through non-local high-emission regions. These local and non-local factors should be considered in future studies of ozone and its mitigation over the plateau. Future work could conduct further TCO analyses, detailed high-resolution CTM simulations, together with statistical and/or artificial intelligence methods, to better quantify the individual and combined effects of various emission and meteorological factors on the TP ozone.

Data availability

The real-time urban surface ozone data are available on the MEE website (http://www.cnemc.cn/en/, last accessed on April 21, 2024). Ozone mixing ratios at the Waliguan station from 2017 to 2019 can be obtained by contacting the co-author Junli

https://doi.org/10.5194/egusphere-2024-3471
Preprint. Discussion started: 25 November 2024

Jin (jinjl@cma.gov.cn). PHLET-OMI anthropogenic NO_x emissions used in this paper are available upon request to the corresponding author Jintai Lin (linjt@pku.edu.cn). All other data used in this study are publicly available and can be downloaded from the following links:

1. Ozone mixing ratios at the Waliguan station from 1994 to 2016 (https://igacproject.org/activities/TOAR, last accessed on April 21, 2024).
2. OMI/MLS TCO product (https://acd-ext.gsfc.nasa.gov/Data_services/cloud_slice/new_data.html, last accessed on April 21, 2024).
3. OMI-RAL and IASI-FORLI TCO products (https://cds.climate.copernicus.eu/cdsapp#!/dataset/satellite-ozone?tab=form, last accessed on April 21, 2024).
4. IASI-SOFRID TCO product (https://thredds.sedoo.fr/iasi-sofrid-o3-co/, last accessed on March 15, 2021).
5. MERRA2 assimilated meteorological data (https://disc.gsfc.nasa.gov/datasets?project=MERRA-2, last accessed on July 17, 2024).
6. CEDS version-2 emissions (https://doi.org/10.25584/PNNLDataHub/1779095, last accessed on July 17, 2024).

Author contributions

JL conceived the study. CX and JL designed the study, analyzed the results, and wrote the paper. HK provided the PHLET-OMI NO_x emission data. XX and JJ analyzed the ozone data at the Waliguan station from 2017 to 2019. LC helped to analyze the simulation results. All authors commented on the manuscript.

Competing interests

The contact author has declared that none of the authors has any competing interests.

Financial support

Jintai Lin and Chenghao Xu have been supported by the National Key Research and Development Program of China (grant no. 2023YFC3705802), the second Tibetan Plateau Scientific Expedition and Research Program (grant no. 2019QZKK0604), and the National Natural Science Foundation of China (grant no. 42430603 and 42075175). Xiaobin Xu has been supported by CAMS Development Fund for Science and Technology (grant no. 2020KJ003). Junli Jin has been supported by the National Natural Science Foundation of China (grant no. 41805027) and the National Key Research and Development Program of China (grant no. 2017YFC1501802).

https://doi.org/10.5194/egusphere-2024-3471
Preprint. Discussion started: 25 November 2024

References

Atkinson, R., Barregård, L., Bellander, T., Burnett, R., Cassee, F., De Oliveira Fernandes, E., Forastiere, F., Forsberg, B., Wothe, S., Hoek, G., Holgate, S., Janssen, N., Jantunen, M., Kelly, F., Lanki, T., Mills, I., Mudway, I., Nieuwenhuijsen, M., Ostro, B., and Williams, M.: Review of evidence on health aspects of air pollution – REVIHAAP Project Technical Report, 2013.

Barret, B., Emili, E., and Le Flochmoen, E.: A tropopause-related climatological a priori profile for IASI-SOFRID ozone retrievals: improvements and validation, Atmospheric Measurement Techniques, 13, 5237-5257, 10.5194/amt-13-5237-2020, 2020.

Boynard, A., Hurtmans, D., Garane, K., Goutail, F., Hadji-Lazaro, J., Koukouli, M. E., Wespes, C., Vigouroux, C., Keppens, A., Pommereau, J.-P., Pazmino, A., Balis, D., Loyola, D., Valks, P., Sussmann, R., Smale, D., Coheur, P.-F., and Clerbaux, C.: Validation of the IASI FORLI/EUMETSAT ozone products using satellite (GOME-2), ground-based (Brewer–Dobson, SAOZ, FTIR) and ozonesonde measurements, Atmospheric Measurement Techniques, 11, 5125-5152, 10.5194/amt-11-5125-2018, 2018.

Boynard, A., Hurtmans, D., Koukouli, M. E., Goutail, F., Bureau, J., Safieddine, S., Lerot, C., Hadji-Lazaro, J., Wespes, C., Pommereau, J.-P., Pazmino, A., Zyrichidou, I., Balis, D., Barbe, A., Mikhailenko, S. N., Loyola, D., Valks, P., Van Roozendael, M., Coheur, P.-F., and Clerbaux, C.: Seven years of IASI ozone retrievals from FORLI: validation with independent total column and vertical profile measurements, Atmospheric Measurement Techniques, 9, 4327-4353, 10.5194/amt-9-4327-2016, 2016.

Chen, S., Wang, W., Li, M., Mao, J., Ma, N., Liu, J., Bai, Z., Zhou, L., Wang, X., Bian, J., and Yu, P.: The Contribution of Local Anthropogenic Emissions to Air Pollutants in Lhasa on the Tibetan Plateau, Journal of Geophysical Research: Atmospheres, 127, 10.1029/2021jd036202, 2022a.

Chen, Y., Lin, W., Xu, X., and Zheng, X.: Surface ozone in southeast Tibet: variations and implications of tropospheric ozone sink over a highland, Environmental Chemistry, 2022b.

Chen, Y., Zhou, Y., NixiaCiren, Zhang, H., Wang, C., GesangDeji, and Wang, X.: Spatiotemporal variations of surface ozone and its influencing factors across Tibet: A Geodetector-based study, Science of The Total Environment, 813, 152651, https://doi.org/10.1016/j.scitotenv.2021.152651, 2022c.

Cohen, M. D., Stunder, B. J. B., Rolph, G. D., Draxler, R. R., Stein, A. F., and Ngan, F.: NOAA's HYSPLIT Atmospheric Transport and Dispersion Modeling System, Bulletin of the American Meteorological Society, 96, 2059-2077, 10.1175/bams-d-14-00110.1, 2015.

Cooper, O. R., Parrish, D. D., Stohl, A., Trainer, M., Nédélec, P., Thouret, V., Cammas, J. P., Oltmans, S. J., Johnson, B. J., Tarasick, D., Leblanc, T., McDermid, I. S., Jaffe, D., Gao, R., Stith, J., Ryerson, T., Aikin, K., Campos, T., Weinheimer, A., and Avery, M. A.: Increasing springtime ozone mixing ratios in the free troposphere over western North America, Nature, 463, 344-348, 10.1038/nature08708, 2010.

Cristofanelli, P., Bracci, A., Sprenger, M., Marinoni, A., Bonafè, U., Calzolari, F., Duchi, R., Laj, P., Pichon, J. M., Roccato, F., Venzac, H., Vuillermoz, E., and Bonasoni, P.: Tropospheric ozone variations at the Nepal Climate Observatory-Pyramid (Himalayas, 5079 m a.s.l.) and influence of deep stratospheric intrusion events, Atmospheric Chemistry and Physics, 10, 6537-6549, 10.5194/acp-10-6537-2010, 2010.

Cui, Y., Lin, J., Song, C., Liu, M., Yan, Y., Xu, Y., and Huang, B.: Rapid growth in nitrogen dioxide pollution over Western China, 2005–2013, Atmos. Chem. Phys., 16, 6207-6221, 10.5194/acp-16-6207-2016, 2016.

Desqueyroux, H., Pujet, J. C., Prosper, M., Squinazi, F., and Momas, I.: Short-term effects of low-level air pollution on respiratory health of adults suffering from moderate to severe asthma, Environ Res, 89, 29-37, 10.1006/enrs.2002.4357, 2002.

Ding, A., Wang, T., and Fu, C.: Transport characteristics and origins of carbon monoxide and ozone in Hong Kong, South China, Journal of Geophysical Research: Atmospheres, 118, 9475-9488, 10.1002/jgrd.50714, 2013.

Ding, T., Gao, H., and Yuan, Y.: The record-breaking northward shift of the western Pacific subtropical high in summer 2018 and the possible role of cross-equatorial flow over the Bay of Bengal, Theoretical and Applied Climatology, 139, 701-710, 10.1007/s00704-019-02997-4, 2019.

https://doi.org/10.5194/egusphere-2024-3471
Preprint. Discussion started: 25 November 2024

Dufour, G., Eremenko, M., Griesfeller, A., Barret, B., LeFlochmoën, E., Clerbaux, C., Hadji-Lazaro, J., Coheur, P. F., and Hurtmans, D.: Validation of three different scientific ozone products retrieved from IASI spectra using ozonesondes, Atmos. Meas. Tech., 5, 611-630, 10.5194/amt-5-611-2012, 2012.

Geng, G. N., Zhang, Q., Martin, R. V., Lin, J. T., Huo, H., Zheng, B., Wang, S. W., and He, K. B.: Impact of spatial proxies on the representation of bottom-up emission inventories: A satellite-based analysis, ATMOSPHERIC CHEMISTRY AND PHYSICS, 17, 4131-4145, 10.5194/acp-17-4131-2017, 2017.

Han, H., Zhang, L., Liu, Z., Yue, X., Shu, L., Wang, X., and Zhang, Y.: Narrowing Differences in Urban and Nonurban Surface Ozone in the Northern Hemisphere Over 1990–2020, Environmental Science & Technology Letters, 10, 410-417, 10.1021/acs.estlett.3c00105, 2023.

Hu, Y., Yu, H., Kang, S., Yang, J., Chen, X., Yin, X., and Chen, P.: Modeling the transport of PM10, PM2.5, and O3 from South Asia to the Tibetan Plateau, Atmospheric Research, 303, 107323, https://doi.org/10.1016/j.atmosres.2024.107323, 2024.

Kalsoom, U., Wang, T., Ma, C., Shu, L., Huang, C., and Gao, L.: Quadrennial variability and trends of surface ozone across China during 2015–2018: A regional approach, Atmospheric Environment, 245, 117989, https://doi.org/10.1016/j.atmosenv.2020.117989, 2021.

Kantha, L. H. and Clayson, C. A.: An improved mixed layer model for geophysical applications, Journal of Geophysical Research: Oceans, 99, 25235-25266, 10.1029/94jc02257, 2012.

Kong, H., Lin, J., Chen, L., Zhang, Y., Yan, Y., Liu, M., Ni, R., Liu, Z., and Weng, H.: Considerable Unaccounted Local Sources of NO(x) Emissions in China Revealed from Satellite, Environ Sci Technol, 56, 7131-7142, 10.1021/acs.est.1c07723, 2022.

Kong, H., Lin, J., Zhang, R., Liu, M., Weng, H., Ni, R., Chen, L., Wang, J., Yan, Y., and Zhang, Q.: High-resolution (0.05° × 0.05°) NO_{<i>x</i>} emissions in the Yangtze River Delta inferred from OMI, Atmospheric Chemistry and Physics, 19, 12835-12856, 10.5194/acp-19-12835-2019, 2019.

Kong, H., Lin, J., Zhang, Y., Li, C., Xu, C., Shen, L., Liu, X., Yang, K., Su, H., and Xu, W.: High natural nitric oxide emissions from lakes on Tibetan Plateau under rapid warming, Nature Geoscience, 16, 474-477, 10.1038/s41561-023-01200-8, 2023.

Li, K., Jacob, D. J., Liao, H., Shen, L., Zhang, Q., and Bates, K. H.: Anthropogenic drivers of 2013–2017 trends in summer surface ozone in China, Proceedings of the National Academy of Sciences, 116, 422-427, 10.1073/pnas.1812168116, 2019.

Li, K., Jacob, D. J., Liao, H., Qiu, Y. L., Shen, L., Zhai, S. X., Bates, K. H., Sulprizio, M. P., Song, S. J., Lu, X., Zhang, Q., Zheng, B., Zhang, Y. L., Zhang, J. Q., Lee, H. C., and Kuk, S. K.: Ozone pollution in the North China Plain spreading into the late-winter haze season, Proc. Natl. Acad. Sci. U. S. A., 118, 7, 10.1073/pnas.2015797118, 2021.

Li, M., Liu, H., Geng, G., Hong, C., Liu, F., Song, Y., Tong, D., Zheng, B., Cui, H., Man, H., Zhang, Q., and He, K.: Anthropogenic emission inventories in China: a review, National Science Review, 4, 834-866, 10.1093/nsr/nwx150, 2017.

Li, Q., Gong, D., Wang, H., Deng, S., Zhang, C., Mo, X., Chen, J., and Wang, B.: Tibetan Plateau is vulnerable to aromatic-related photochemical pollution and health threats: A case study in Lhasa, Science of The Total Environment, 904, 166494, https://doi.org/10.1016/j.scitotenv.2023.166494, 2023a.

Li, W., Han, X., Li, J., Lun, X., and Zhang, M.: Assessment of surface ozone production in Qinghai, China with satellite-constrained VOCs and NOx emissions, Science of The Total Environment, 905, 166602, https://doi.org/10.1016/j.scitotenv.2023.166602, 2023b.

Lin, J.-T. and McElroy, M. B.: Impacts of boundary layer mixing on pollutant vertical profiles in the lower troposphere: Implications to satellite remote sensing, Atmospheric Environment, 44, 1726-1739, https://doi.org/10.1016/j.atmosenv.2010.02.009, 2010.

Lin, J. T., Liu, M. Y., Xin, J. Y., Boersma, K. F., Spurr, R., Martin, R., and Zhang, Q.: Influence of aerosols and surface reflectance on satellite NO₂ retrieval: seasonal and spatial characteristics and implications for NO_x emission constraints, Atmospheric Chemistry and Physics, 15, 11217-11241, 10.5194/acp-15-11217-2015, 2015a.

Lin, J. T., Martin, R. V., Boersma, K. F., Sneep, M., Stammes, P., Spurr, R., Wang, P., Van Roozendael, M., Clémer, K., and Irie, H.: Retrieving tropospheric nitrogen dioxide from the Ozone Monitoring Instrument: effects of aerosols, surface reflectance anisotropy, and vertical profile of nitrogen dioxide, Atmos. Chem. Phys., 14, 1441-1461, 10.5194/acp-14-1441-2014, 2014.

https://doi.org/10.5194/egusphere-2024-3471
Preprint. Discussion started: 25 November 2024

Lin, W., Xu, X., Zheng, X., Dawa, J., Baima, C., and Ma, J.: Two-year measurements of surface ozone at Dangxiong, a remote highland site in the Tibetan Plateau, Journal of Environmental Sciences, 31, 133-145, https://doi.org/10.1016/j.jes.2014.10.022, 2015b.

Liu, M., Lin, J., Boersma, K. F., Pinardi, G., Wang, Y., Chimot, J., Wagner, T., Xie, P., Eskes, H., Van Roozendael, M., Hendrick, F., Wang, P., Wang, T., Yan, Y., Chen, L., and Ni, R.: Improved aerosol correction for OMI tropospheric NO₂ retrieval over East Asia: constraint from CALIOP aerosol vertical profile, Atmospheric Measurement Techniques, 12, 1-21, 10.5194/amt-12-1-2019, 2019.

Liu, Y. and Wang, T.: Worsening urban ozone pollution in China from 2013 to 2017 – Part 1: The complex and varying roles of meteorology, Atmospheric Chemistry and Physics, 20, 6305-6321, 10.5194/acp-20-6305-2020, 2020a.

Liu, Y. and Wang, T.: Worsening urban ozone pollution in China from 2013 to 2017 – Part 2: The effects of emission changes and implications for multi-pollutant control, Atmospheric Chemistry and Physics, 20, 6323-6337, 10.5194/acp-20-6323-2020, 2020b.

Liu, Y., Geng, G., Cheng, J., Liu, Y., Xiao, Q., Liu, L., Shi, Q., Tong, D., He, K., and Zhang, Q.: Drivers of Increasing Ozone during the Two Phases of Clean Air Actions in China 2013–2020, Environmental Science & Technology, 57, 8954-8964, 10.1021/acs.est.3c00054, 2023a.

Liu, Y., Geng, G., Cheng, J., Liu, Y., Xiao, Q., Liu, L., Shi, Q., Tong, D., He, K., and Zhang, Q.: Drivers of Increasing Ozone during the Two Phases of Clean Air Actions in China 2013–2020, Environmental Science & Technology, 57, 8954-8964, 10.1021/acs.est.3c00054, 2023b.

Lu, X., Zhang, L., Wang, X., Gao, M., Li, K., Zhang, Y., Yue, X., and Zhang, Y.: Rapid Increases in Warm-Season Surface Ozone and Resulting Health Impact in China Since 2013, Environmental Science & Technology Letters, 7, 240-247, 10.1021/acs.estlett.0c00171, 2020.

Lu, X., Hong, J., Zhang, L., Cooper, O. R., Schultz, M. G., Xu, X., Wang, T., Gao, M., Zhao, Y., and Zhang, Y.: Severe Surface Ozone Pollution in China: A Global Perspective, Environmental Science & Technology Letters, 5, 487-494, 10.1021/acs.estlett.8b00366, 2018.

Lu, X., Zhang, L., Chen, Y., Zhou, M., Zheng, B., Li, K., Liu, Y., Lin, J., Fu, T. M., and Zhang, Q.: Exploring 2016–2017 surface ozone pollution over China: source contributions and meteorological influences, Atmos. Chem. Phys., 19, 8339-8361, 10.5194/acp-19-8339-2019, 2019.

Ma, J., Lin, W. L., Zheng, X. D., Xu, X. B., Li, Z., and Yang, L. L.: Influence of air mass downward transport on the variability of surface ozone at Xianggelila Regional Atmosphere Background Station, southwest China, Atmospheric Chemistry and Physics, 14, 5311-5325, 10.5194/acp-14-5311-2014, 2014.

Ma, J., Zhou, X., Xu, X., Xu, X., Gromov, S., and Lelieveld, J.: Chapter 15 - Ozone and aerosols over the Tibetan Plateau, in: Asian Atmospheric Pollution, edited by: Singh, R. P., Elsevier, 287-302, https://doi.org/10.1016/B978-0-12-816693-2.00008-1, 2022.

Marinoni, A., Cristofanelli, P., Laj, P., Duchi, R., Putero, D., Calzolari, F., Landi, T. C., Vuillermoz, E., Maione, M., and Bonasoni, P.: High black carbon and ozone concentrations during pollution transport in the Himalayas: Five years of continuous observations at NCO-P global GAW station, Journal of Environmental Sciences, 25, 1618-1625, 10.1016/s1001-0742(12)60242-3, 2013.

Matricardi, M., Chevallier, F., Kelly, G., and Thépaut, J.-N.: An improved general fast radiative transfer model for the assimilation of radiance observations, Quarterly Journal of the Royal Meteorological Society, 130, 153-173, 10.1256/qj.02.181, 2004.

Mauzerall, D. L. and Wang, X.: PROTECTINGAGRICULTURALCROPS FROM THEEFFECTS OFTROPOSPHERICOZONEEXPOSURE: Reconciling Science and Standard Setting in the United States, Europe, and Asia, Annual Review of Energy and the Environment, 26, 237-268, 10.1146/annurev.energy.26.1.237, 2001.

Miles, G. M., Siddans, R., Kerridge, B. J., Latter, B. G., and Richards, N. A. D.: Tropospheric ozone and ozone profiles retrieved from GOME-2 and their validation, Atmospheric Measurement Techniques, 8, 385-398, 10.5194/amt-8-385-2015, 2015.

Ni, R., Lin, J., Yan, Y., and Lin, W.: Foreign and domestic contributions to springtime ozone over China, Atmospheric Chemistry and Physics, 18, 11447-11469, 10.5194/acp-18-11447-2018, 2018.

https://doi.org/10.5194/egusphere-2024-3471
Preprint. Discussion started: 25 November 2024

Ni, Y., Yang, Y., Wang, H., Li, H., Li, M., Wang, P., Li, K., and Liao, H.: Contrasting changes in ozone during 2019–2021 between eastern and the other regions of China attributed to anthropogenic emissions and meteorological conditions, Science of The Total Environment, 908, 168272, https://doi.org/10.1016/j.scitotenv.2023.168272, 2024.

O'Rourke, P. R. S., S. J.; Mott, A.; Ahsan, H.; McDuffie, E. E.; Crippa, M.; Klimont, S.; McDonald, B.; Z., Wang; Nicholson, M. B; Feng, L.; and Hoesly, R. M.: CEDS v-2021-02-05 Emission Data 1975-2019 (Feb-05-2021) [dataset], 10.5281/zenodo.4509372., 2021.

Pan, W., Gong, S., Lu, K., Zhang, L., Xie, S., Liu, Y., Ke, H., Zhang, X., and Zhang, Y.: Multi-scale analysis of the impacts of meteorology and emissions on PM2.5 and O3 trends at various regions in China from 2013 to 2020 3. Mechanism assessment of O3 trends by a model, Science of The Total Environment, 857, 159592, https://doi.org/10.1016/j.scitotenv.2022.159592, 2023.

Putero, D., Landi, T. C., Cristofanelli, P., Marinoni, A., Laj, P., Duchi, R., Calzolari, F., Verza, G. P., and Bonasoni, P.: Influence of open vegetation fires on black carbon and ozone variability in the southern Himalayas (NCO-P, 5079 m a.s.l.), Environmental Pollution, 184, 597-604, 10.1016/j.envpol.2013.09.035, 2014.

Ran, L., Lin, W. L., Deji, Y. Z., La, B., Tsering, P. M., Xu, X. B., and Wang, W.: Surface gas pollutants in Lhasa, a highland city of Tibet – current levels and pollution implications, Atmospheric Chemistry and Physics, 14, 10721-10730, 10.5194/acp-14-10721-2014, 2014.

Stohl, A.: A backward modeling study of intercontinental pollution transport using aircraft measurements, Journal of Geophysical Research, 108, 10.1029/2002jd002862, 2003.

Tan, W., Wang, H., Su, J., Sun, R., He, C., Lu, X., Lin, J., Xue, C., Wang, H., Liu, Y., Liu, L., Zhang, L., Wu, D., Mu, Y., and Fan, S.: Soil Emissions of Reactive Nitrogen Accelerate Summertime Surface Ozone Increases in the North China Plain, Environmental Science & Technology, 57, 12782-12793, 10.1021/acs.est.3c01823, 2023.

Wang, J., Ge, B., and Wang, Z.: Ozone Production Efficiency in Highly Polluted Environments, Current Pollution Reports, 4, 198-207, 10.1007/s40726-018-0093-9, 2018.

Wang, M., Chen, X., Jiang, Z., He, T.-L., Jones, D., Liu, J., and Shen, Y.: Meteorological and anthropogenic drivers of surface ozone change in the North China Plain in 2015–2021, Science of The Total Environment, 906, 167763, https://doi.org/10.1016/j.scitotenv.2023.167763, 2024.

Wang, T., Dai, J., Lam, K. S., Nan Poon, C., and Brasseur, G. P.: Twenty-Five Years of Lower Tropospheric Ozone Observations in Tropical East Asia: The Influence of Emissions and Weather Patterns, Geophysical Research Letters, 46, 11463-11470, 10.1029/2019gl084459, 2019.

Warneck: Chemistry of the natural atmosphere, Chemistry of the natural atmosphere /1999.

Weng, H., Lin, J., Martin, R., Millet, D. B., Jaeglé, L., Ridley, D., Keller, C., Li, C., Du, M., and Meng, J.: Global high-resolution emissions of soil NOx, sea salt aerosols, and biogenic volatile organic compounds, Scientific Data, 7, 148, 10.1038/s41597-020-0488-5, 2020.

Weng, X., Forster, G. L., and Nowack, P.: A machine learning approach to quantify meteorological drivers of ozone pollution in China from 2015 to 2019, Atmospheric Chemistry and Physics, 22, 8385-8402, 10.5194/acp-22-8385-2022, 2022.

Wu, S., Mickley, L. J., Jacob, D. J., Logan, J. A., Yantosca, R. M., and Rind, D.: Why are there large differences between models in global budgets of tropospheric ozone?, Journal of Geophysical Research: Atmospheres, 112, 10.1029/2006jd007801, 2007.

Xu, H., Yu, H., Xu, B., Wang, Z., Wang, F., Wei, Y., Liang, W., Liu, J., Liang, D., Feng, Y., and Shi, G.: Machine learning coupled structure mining method visualizes the impact of multiple drivers on ambient ozone, Communications Earth & Environment, 4, 10.1038/s43247-023-00932-0, 2023.

Xu, W., Lin, W., Xu, X., Tang, J., Huang, J., Wu, H., and Zhang, X.: Long-term trends of surface ozone and its influencing factors at the Mt Waliguan GAW station, China – Part 1: Overall trends and characteristics, Atmospheric Chemistry and Physics, 16, 6191-6205, 10.5194/acp-16-6191-2016, 2016.

Xu, W., Xu, X., Lin, M., Lin, W., Tarasick, D., Tang, J., Ma, J., and Zheng, X.: Long-term trends of surface ozone and its influencing factors at the Mt Waliguan GAW station, China – Part 2: The roles of anthropogenic emissions and climate variability, Atmospheric Chemistry and Physics, 18, 773-798, 10.5194/acp-18-773-2018, 2018a.

https://doi.org/10.5194/egusphere-2024-3471
Preprint. Discussion started: 25 November 2024

Xu, X., Zhang, H., Lin, W., Wang, Y., Xu, W., and Jia, S.: First simultaneous measurements of peroxyacetyl nitrate (PAN) and ozone at Nam Co in the central Tibetan Plateau: impacts from the PBL evolution and transport processes, Atmospheric Chemistry and Physics, 18, 5199-5217, 10.5194/acp-18-5199-2018, 2018b.

Xu, X., Lin, W., Xu, W., Jin, J., Wang, Y., Zhang, G., Zhang, X., Ma, Z., Dong, Y., Ma, Q., Yu, D., Li, Z., Wang, D., and Zhao, H.: Long-term changes of regional ozone in China: implications for human health and ecosystem impacts, Elementa: Science of the Anthropocene, 8, 10.1525/elementa.409, 2020.

Xue, L. K., Wang, T., Zhang, J. M., Zhang, X. C., Deliger, Poon, C. N., Ding, A. J., Zhou, X. H., Wu, W. S., Tang, J., Zhang, Q. Z., and Wang, W. X.: Source of surface ozone and reactive nitrogen speciation at Mount Waliguan in western China: New insights from the 2006 summer study, Journal of Geophysical Research, 116, 10.1029/2010jd014735, 2011.

Yan, Y., Lin, J., and He, C.: Ozone trends over the United States at different times of day, Atmos. Chem. Phys., 18, 1185-1202, 10.5194/acp-18-1185-2018, 2018a.

Yan, Y., Lin, J., Chen, J., and Hu, L.: Improved simulation of tropospheric ozone by a global-multi-regional two-way coupling model system, Atmos. Chem. Phys., 16, 2381-2400, 10.5194/acp-16-2381-2016, 2016.

Yan, Y., Pozzer, A., Ojha, N., Lin, J., and Lelieveld, J.: Analysis of European ozone trends in the period 1995–2014, Atmos. Chem. Phys., 18, 5589-5605, 10.5194/acp-18-5589-2018, 2018b.

Yang, J., Kang, S., Hu, Y., Chen, X., and Rai, M.: Influence of South Asian Biomass Burning on Ozone and Aerosol Concentrations Over the Tibetan Plateau, Advances in Atmospheric Sciences, 39, 1184-1197, 10.1007/s00376-022-1197-0, 2022.

Ye, X., Zhang, L., Wang, X., Lu, X., Jiang, Z., Lu, N., Li, D., and Xu, J.: Spatial and temporal variations of surface background ozone in China analyzed with the grid-stretching capability of GEOS-Chem High Performance, Science of The Total Environment, 914, 169909, https://doi.org/10.1016/j.scitotenv.2024.169909, 2024.

Yin, H., Sun, Y., Notholt, J., Palm, M., Ye, C., and Liu, C.: Quantifying the drivers of surface ozone anomalies in the urban areas over the Qinghai-Tibet Plateau, Atmospheric Chemistry and Physics, 22, 14401-14419, 10.5194/acp-22-14401-2022, 2022.

Yin, X., Kang, S., de Foy, B., Cong, Z., Luo, J., Zhang, L., Ma, Y., Zhang, G., Rupakheti, D., and Zhang, Q.: Surface ozone at Nam Co in the inland Tibetan Plateau: variation, synthesis comparison and regional representativeness, Atmospheric Chemistry and Physics, 17, 11293-11311, 10.5194/acp-17-11293-2017, 2017.

Yuan, Y., Gao, H., and Ding, T.: The extremely north position of the western Pacific subtropical high in summer of 2018: Important role of the convective activities in the western Pacific, International Journal of Climatology, 40, 1361-1374, 10.1002/joc.6274, 2019.

Zhang, Y., Lin, J., Liu, M., Kong, H., Chen, L., Weng, H., and Li, C.: High-resolution Tropospheric NO₂ Retrieval over Asia based on OMI POMINO v2.1 and quantitative comparison with other products, National Remote Sensing Bulletin, 26, 971-987, 10.11834/jrs.20221413, 2022.

Zhao, H., Li, X., Zhang, Q., Jiang, X., Lin, J., Peters, G. P., Li, M., Geng, G., Zheng, B., Huo, H., Zhang, L., Wang, H., Davis, S. J., and He, K.: Effects of atmospheric transport and trade on air pollution mortality in China, Atmos. Chem. Phys., 17, 10367-10381, 10.5194/acp-17-10367-2017, 2017.

Zheng, B., Tong, D., Li, M., Liu, F., Hong, C., Geng, G., Li, H., Li, X., Peng, L., Qi, J., Yan, L., Zhang, Y., Zhao, H., Zheng, Y., He, K., and Zhang, Q.: Trends in China's anthropogenic emissions since 2010 as the consequence of clean air actions, Atmospheric Chemistry and Physics, 18, 14095-14111, 10.5194/acp-18-14095-2018, 2018.

Zheng, D. and Shi, M.: Multiple environmental policies and pollution haven hypothesis: Evidence from China's polluting industries, Journal of Cleaner Production, 141, 295-304, https://doi.org/10.1016/j.jclepro.2016.09.091, 2017.

Zheng, H., Kong, S., He, Y., Song, C., Cheng, Y., Yao, L., Chen, N., and Zhu, B.: Enhanced ozone pollution in the summer of 2022 in China: The roles of meteorology and emission variations, Atmospheric Environment, 301, 119701, https://doi.org/10.1016/j.atmosenv.2023.119701, 2023.

Zhu, T., Lin, W., Song, Y., Cai, X., Zou, H., Kang, L., Zhou, L., and Akimoto, H.: Downward transport of ozone-rich air near Mt. Everest, Geophysical Research Letters, 33, 10.1029/2006gl027726, 2006.

Ziemke, J. R., Chandra, S., and Bhartia, P. K.: "Cloud slicing": A new technique to derive upper tropospheric ozone from satellite measurements, Journal of Geophysical Research: Atmospheres, 106, 9853-9867, https://doi.org/10.1029/2000JD900768, 2001.

https://doi.org/10.5194/egusphere-2024-3471
Preprint. Discussion started: 25 November 2024

Ziemke, J. R., Chandra, S., Labow, G. J., Bhartia, P. K., Froidevaux, L., and Witte, J. C.: A global climatology of tropospheric and stratospheric ozone derived from Aura OMI and MLS measurements, Atmospheric Chemistry and Physics, 11, 9237-9251, 10.5194/acp-11-9237-2011, 2011.

Ziemke, J. R., Chandra, S., Duncan, B. N., Froidevaux, L., Bhartia, P. K., Levelt, P. F., and Waters, J. W.: Tropospheric ozone determined from Aura OMI and MLS: Evaluation of measurements and comparison with the Global Modeling Initiative's Chemical Transport Model, Journal of Geophysical Research, 111, 10.1029/2006jd007089, 2006.